AIAA JOURNAL
Vol. 33, No. 10, October 1995

Direct Strain Measure for Large-Deformation Analyses of Beam Structures

Jin Mitsugi*
NTT Radio Communication Systems Laboratories, Yokosuka 238-03, Japan

A nonlinear kinematics called the direct strain measure is proposed for large deformation and finite rotation analyses of a two-node Timoshenko beam. The kinematics extracts pure elastic deformations without deriving any virtual frame to describe rigid body motion. Internal force and stiffness matrices are derived to constitute a Newton's method for finding the solution. Computational results show that the present method is valid for Timoshenko beams whose relative angular displacement in an element is less than 0.5 rad.

I. Introduction

MANY types of space structures involve beams as structural components. In single-beam applications, such as space tethers and wire antennas, the beam is long and, therefore, flexible. As such, it would be difficult to presume that the deformation of the beam is infinitesimally small. Consequently, linear analysis is not applicable. This is also true for beams in truss structure type applications when deployments or slewing maneuver types of motions are applied. As such, a precision analysis on beam structures must have the capability to handle large deformations. Even if the deformation is large, the resultant strains can be assumed to be small in most practical applications.

The difficulty of analyzing beams exhibiting large deformation but small strain stems from the need to derive a kinematics (displacement-strain relation) valid for large deformations and finite rotations. Atluri,[1] Iura and Atluri,[2,3] and Crivelli[4] employed the Green strain tensor for analyses. References 5–7 used a convected frame to describe the strain tensor. Hodges[8] used polar decomposition to eliminate the rigid body rotation and applied the Jaumann–Biot–Cauchy strain tensor. Using these tensor analyses, special attention must be paid to the physical interpretation of tensor elements. Different from the tensor oriented approach, in Refs. 9–11 a method is presented in which the strains are measured from a virtual frame which is assumed to describe the rigid body motion of elements. Rankin and Brogen[12] presented the projector matrix method to extract pure elastic deformation. These corotational methods give direct physical interpretation of the analytic process. The core issue in the corotational methods is the validity of the corotational frame.

In the course of developing a simple method to generate an accurate corotational frame, the author found the possibility of extracting pure strains without introducing any corotational frame. The motivation was a large-deformation analysis of rod elements. The elongation strain ϵ_{xx} of largely deformed rod element is given[13] as

$$\epsilon_{xx} = (|\boldsymbol{X}_2 - \boldsymbol{X}_1| - L)/L \tag{1}$$

where $\boldsymbol{X}_1$ and $\boldsymbol{X}_2$ are the terminal positions of the rod element in the inertial frame and L is the undeformed length of the element. In this case, the strain is measured from the deformed geometry without introducing any virtual frame. This is the basic concept of the direct strain measure (DSM). It is, of course, possible to measure the elongation strain after setting up a corotational virtual frame, but an unnecessary ambiguity occurs at the determination of the frames perpendicular to the rod orientation.

This paper presents a finite element method based on DSM for a two-node Timoshenko beam model. The paper is organized in the following manner. In Sec. II, strains determined with DSM are presented. In Sec. III, the first and second variations of strain are derived to yield the internal force and the tangent stiffness matrices. They are used to determine the equilibrium condition using Newton's method for solution finding. Computational examples are presented in Sec. IV to demonstrate the basic performance of the proposed method.

Received April 28, 1994; revision received March 13, 1995; accepted for publication March 13, 1995.

*Senior Research Engineer, Satellite Communication Systems Department, 1-2356 Take. Member AIAA.

II. Nonlinear Kinematics Using Direct Strain Measure

This section deals with the kinematics of DSM for two-node Timoshenko beams subjected to small strain and large deformation. The deformed geometry of a beam is described in terms of nodal displacement and finite rotation. Warping of the cross section is not taken into consideration. In the proceeding subsections, it will be eventually shown that four strain components, elongation, bending, torsion, and transverse shears, for a Timoshenko beam can be derived without introducing a virtual frame to describe the rigid body motion of beam elements.

A. Geometry Definition

Three coordinate frames are introduced for the formulation: global, elemental, and nodal frames. The global frame is fixed to the inertial space. Translational displacements of the node are described in this frame. The elemental frame is fixed to the element to describe an arbitrary material position in an element. It should be noted that the relation between the global and the elemental frame after deformation need not to be established when DSM is employed. The nodal frame is fixed to each node. It is assumed that the elemental and nodal frames coincide only at the initial state. The initial elemental and nodal x axes parallel the element's longitudinal axis (Fig. 1). For brevity, it is also assumed in the following formulation that the initial elemental frame coincides with the global frame, but this is not a requirement for the formulation. Let $\boldsymbol{X}_i$, $Q_i (i = 1, 2)$, and ξ denote the terminal nodes position vector after deformation in the global frame, the Euler parameter for the terminal nodes to describe the rotational transformation from the initial nodal frame to the deformed orientation, and the cross-sectional coordinate in the elemental frame, respectively. The cross-sectional coordinate is generalized as

$$\xi = \begin{Bmatrix} 0 \\ \zeta \\ \eta \end{Bmatrix} \tag{2}$$

The Euler parameter Q_i has four components such that

$$Q_i = \begin{Bmatrix} q_0^i \\ q_1^i \\ q_2^i \\ q_3^i \end{Bmatrix} \tag{3}$$

and has the norm constraint of $Q_i^T Q_i = 1$.

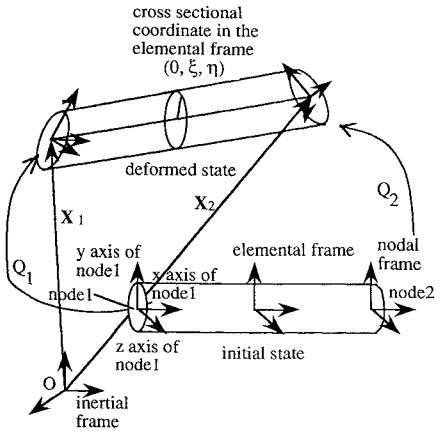

Fig. 1 Geometry definitions for the formulation.

B. Elongation Strain

Defining the nonstressed length of element as L, the elongation strain of the element centroid is given as follows:

$$\epsilon_a = (|X_2 - X_1| - L)/L \tag{4}$$

where $|\ |$ denotes the second norm of a vector.

C. Bending and Torsional Strain

Since bending and torsional strains are structural interpretations of local curvatures, efforts have been made to extract local curvatures from the current geometry of the elements. Since small strain and large deformation are assumed, it is valid to stipulate that two nodal Euler parameters in an element have little difference so that the linear interpolation of the Euler parameters furnishes a good approximation for rotations in midspan of the element such that

$$Q(x) = (1 - x/L)Q_1 + (x/L)Q_2 \tag{5}$$

where x denotes the local coordinate spanning from 0 to L. Using Eq. (5), the norm of the Euler parameters at midpoint, $n(x)$, is given as follows:

$$n(x) = Q(x)^T Q(x) \tag{6}$$

$$n(x) = 1 + 2(x/L)\left(Q_1^T Q_2 - 1\right) + x^2/L^2\{Q_2 - Q_1\}^T\{Q_2 - Q_1\} \tag{7}$$

Q_2 can be denoted as the sum of Q_1 and small deviation Δd such that

$$Q_2 = Q_1 + \Delta d \tag{8}$$

Vanishing the second-order terms of Δd and recalling the norm constraint for the Euler parameters, Eq. (7) leads to

$$n(x) \approx 1 \tag{9}$$

The linear interpolation of the Euler parameters is confirmed to be valid. In practical analyses, however, numerical normalization is necessary because the approximation is only valid in the linear sense, whereas actual computation entails the effect of higher order terms and roundoff errors.

The curvature vector κ is obtained by differentiating the rotational matrix $R(x)$ with respect to the axial coordinate x such that

$$\tilde{\kappa} = R^T \frac{\partial R}{\partial x} \tag{10}$$

where the tilde denotes the skew-symmetric matrix. If the rotational matrix is described by using the Euler parameter, the curvature, κ, could be given in a vector form such that

$$\kappa = G\frac{\partial Q}{\partial x} \tag{11}$$

where the G matrix represents the following linear matrix for the Euler parameter components[14]:

$$G = 2\begin{bmatrix} -q_1 & q_0 & q_3 & -q_2 \\ -q_2 & -q_3 & q_0 & q_1 \\ -q_3 & q_2 & -q_1 & q_0 \end{bmatrix} \tag{12}$$

Substituting the linear interpolation of the Euler parameter (5) into the curvature definition (11) and after algebraic manipulations, the curvature vector κ is given in a simple form as

$$\kappa_1 = 2/L\left(-q_1^1 q_0^2 + q_0^1 q_1^2 - q_3^1 q_2^2 + q_2^1 q_3^2\right) \tag{13}$$

$$\kappa_2 = 2/L\left(-q_2^1 q_0^2 + q_0^1 q_2^2 - q_1^1 q_3^2 - q_3^1 q_1^2\right) \tag{14}$$

$$\kappa_3 = 2/L\left(-q_3^1 q_0^2 + q_0^1 q_3^2 - q_2^1 q_1^2 + q_1^1 q_2^2\right) \tag{15}$$

where κ_1, κ_2, and κ_3 denote the torsional curvature and two transverse bending curvatures, respectively. It should be noted that each curvature component only includes the Euler parameters of the terminal nodes, and the resultant curvature is constant through the element span. This constant curvature is only attained by linearly interpolated Euler parameters to represent rotation in midspan. The bending strain ϵ_b is, therefore, given as

$$\epsilon_b = h_1^T \tilde{\xi}^T \kappa \tag{16}$$

where $h_1^T = \{1, 0, 0\}$. Torsional shear strains ϵ_{xy}^t and ϵ_{xz}^t are given as follows:

$$\epsilon_{xy}^t = -\kappa_1 \eta \tag{17}$$

$$\epsilon_{xz}^t = \kappa_1 \zeta \tag{18}$$

D. Transverse Shear

Since transverse shear strain denotes the angle between the elemental centroid and the crosssection minus $\pi/2$, the terminal transverse shear ϵ_{xy}^s is given by the inner product of the normalized centroid vector s

$$s = \frac{X_2 - X_1}{|X_2 - X_1|} \tag{19}$$

and a normal vector attached to the local y axis of the cross section $R_i h_2$ such that

$$\epsilon_{xy}^s\big|_i = s^T R_i h_2 \tag{20}$$

where $h_2 = \{0, 1, 0\}$. Graphycal illustration is given in Fig. 2. Similarly, the other transverse shear strain at the node is given as follows:

$$\epsilon_{xz}^s\big|_i = s^T R_i h_3 \tag{21}$$

Transverse shear strain at the midspan of the element is derived by linearly interpolating the terminal transverse shear strains,

$$\epsilon_{xy}^s = (1 - x/L)s^T R_1 h_2 + (x/L)s^T R_2 h_2 \tag{22}$$

$$\epsilon_{xz}^s = (1 - x/L)s^T R_1 h_3 + (x/L)s^T R_2 h_3 \tag{23}$$

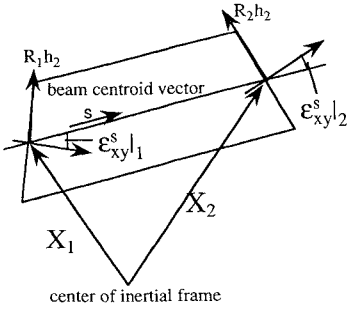

Fig. 2 Physical interpretation of transverse shear.

Since the shear strains obtained from Eqs. (22) and (23) are excessively stiff for thin beams, known as shear locking in low-order elements, one point Gaussian integration is used to compute the internal force and stiffness matrix.

E. Kinematics of the Directly Measured Strains

The strain components for the Timoshenko beam using DSM are summarized as follows:

$$\epsilon_{xx} = \epsilon_a + \epsilon_b = h_1^T \tilde{\xi}^T \kappa + (|X_2 - X_1| - L)/L \tag{24}$$

$$\epsilon_{xy} = \epsilon_{xy}^t + \epsilon_{xy}^s = -\kappa_1 \eta + (1 - x/L) s^T R_1 h_2 + (x/L) s^T R_2 h_2 \tag{25}$$

$$\epsilon_{xz} = \epsilon_{xz}^t + \epsilon_{xz}^s = \kappa_1 \zeta + (1 - x/L) s^T R_1 h_3 + (x/L) s^T R_2 h_3 \tag{26}$$

It should be noted that DSM computes the physical strains directly from the deformed geometry of an element.

III. Internal Force and Stiffness Matrix Derivation

The internal force due to elastic deformation and tangent stiffness matrix are necessary if we are to employ Newton's method to find either static or dynamic solutions. This section deals with the derivation of elemental internal force and stiffness matrix.

A. Elemental Internal Force

Denoting generalized strain as ϵ, the strain energy stored in an element is given in a quadratic form as

$$\pi = \int_v \frac{1}{2} E \epsilon^2 \, dv \tag{27}$$

where E denotes the generalized elastic modulus and $\int_v$ denotes the integration over an element. For the case of axial strain ϵ_{xx}, the potential energy is given as

$$\pi_{xx} = \int_v \frac{E}{2} \epsilon_{xx}^2 \, dv = \int_v \frac{E}{2} \left(h_1^T \tilde{\xi}^T \kappa + \frac{|X_2 - X_1| - L}{L} \right)^2 dv \tag{28}$$

The internal force of an element, denoted as $\delta\pi$, is derived as the variation of the strain energy such that

$$\delta\pi = \int_v E \epsilon \delta\epsilon \, dv \tag{29}$$

In the case of axial strain ϵ_{xx}, the first variation $\delta\epsilon_{xx}$ is given as the variation with respect to the translational displacement X and the curvature κ

$$\delta\epsilon_{xx} = \{\delta X_1 \quad \delta X_2 \quad \delta\kappa\} \begin{Bmatrix} -\frac{1}{L} s \\ \frac{1}{L} s \\ \tilde{\xi} h_1 \end{Bmatrix} \tag{30}$$

where s denotes the normalized vector orienting beam centroid,

$$s = (X_2 - X_1)/(|X_2 - X_1|) \tag{31}$$

The variation of the curvature is separated to the terminal rotational variations $\delta\theta_1$ and $\delta\theta_2$ such that

$$\delta\kappa = \frac{1}{L} [-G_2 \quad G_1] \begin{Bmatrix} \delta Q_1 \\ \delta Q_2 \end{Bmatrix} = \frac{1}{L} [-G_2 \quad G_1] \begin{Bmatrix} \frac{G_1^T}{4} \delta\theta_1 \\ \frac{G_2^T}{4} \delta\theta_2 \end{Bmatrix} \tag{32}$$

The transformation

$$\delta Q_i = \left(G_i^T / 4 \right) \delta\theta_i \tag{33}$$

is derived in Nikravesh.[15] Similar procedures are taken to derive the internal forces due to the transverse shears.

B. Tangent Stiffness Matrix

From the variation of the generalized internal force [Eq. (29)], the tangent stiffness matrix can be derived as

$$\delta^2\pi = \int_v E(\delta\epsilon\delta\epsilon + \delta^2\epsilon\epsilon) \, dv \tag{34}$$

It should be noted that the first and the second terms in Eq. (34) denote the material and the geometric stiffness, respectively. Since $\delta\epsilon$ in Eq. (34) has already obtained in the internal force derivations, attention is focused on the derivation of the second variation of strain $\delta^2\epsilon$ in the geometric stiffness. Since the basic derivations for elongation strain related stiffness matrix and transverse shear related stiffness matrix are similar, the derivation is presented only for the elongation strain ϵ_{xx} related stiffness matrix.

From the definition of the variation of the elongation strain [Eq. (30)], the second variation of the elongation strain is given as follows:

$$\delta^2\epsilon_{xx} = \left\{\delta X_1^T \quad \delta X_2^T \quad \delta\kappa^T\right\} \begin{Bmatrix} -\frac{1}{L}\delta s \\ \frac{1}{L}\delta s \\ 0 \end{Bmatrix} + \left\{\delta^2 X_1^T \quad \delta^2 X_2^T \quad \delta^2\kappa^T\right\} \begin{Bmatrix} -\frac{1}{L} s \\ \frac{1}{L} s \\ \tilde{\xi} h_1 \end{Bmatrix} \tag{35}$$

The following subsections elaborate on the geometric stiffness derived from each of the two terms in Eq. (35), namely, the tension stabilizing stiffness and bending stabilizing stiffness. The reason for the nomenclature is explained in the following subsections.

1. *Tension Stabilizing Stiffness*

After a simple algebraic operation, the variation of the segment vector δs that appeared in Eq. (35) is given as follows:

$$\delta s = \frac{1}{|X_2 - X_1|} [I - ss^T] \{\delta X_2 - \delta X_1\} \tag{36}$$

A transformation matrix X_n is introduced as follows:

$$X_n = \frac{1}{|X_2 - X_1|} [I - ss^T] \tag{37}$$

The first geometric stiffness K_{xx}^{Gt} is, therefore, derived as follows:

$$K_{xx}^{Gt} = \left\{\delta X_1^T \quad \delta X_2^T \quad \delta\kappa^T\right\} \times \int_L E \begin{bmatrix} \frac{A}{L}\epsilon_a X_n & -\frac{A}{L}\epsilon_a X_n & 0 \\ -\frac{A}{L}\epsilon_a X_n & \frac{A}{L}\epsilon_a X_n & 0 \\ 0 & 0 & 0 \end{bmatrix} dx \begin{Bmatrix} \delta X_1 \\ \delta X_2 \\ \delta\kappa \end{Bmatrix} \tag{38}$$

where ϵ_a denotes the centroid elongation of the element,

$$\epsilon_a = (|X_2 - X_1| - L)/L \tag{39}$$

It should be noted here that the stiffness matrix depends on the elongation of the centroid ϵ_a so that this geometric stiffness represents the tensioning effect on the beam element.

2. *Bending Stabilizing Stiffness*

Since the second variation of the translational variables are equal to zero, the remaining problem is the derivation of second variation of the curvature vector. The first variation of the curvature vector [Eq. (32)] is expanded to derive the second variation

$$\delta\kappa = -\frac{G_2 G_1^T}{4L}\delta\theta_1 + \frac{G_1 G_2^T}{4L}\delta\theta_2 \tag{40}$$

The second variation is derived in a straightforward manner such that

$$\delta^2\kappa = -\frac{\delta G_2 G_1^T}{4L}\delta\theta_1 - \frac{\delta G_1 G_2^T}{4L}\delta\theta_1 + \frac{\delta G_1 G_2^T}{4L}\delta\theta_1 + \frac{G_1 \delta G_2^T}{4L}\delta\theta_2 \tag{41}$$

In order to write the stiffness matrix in a quadratic form, a three-dimensional internal force vector $\boldsymbol{F}$ is multiplied from the right-hand side of Eq. (41) and the equation is modified as

$$\delta^2\kappa = \delta\theta_1^T\left\{-\frac{G_1 V_T(\boldsymbol{F}) G_1^T}{16L}\delta\theta_2 - \frac{V\left(G_2^T\boldsymbol{F}\right)G_1^T}{16L}\delta\theta_1\right\}$$

$$+\delta\theta_2^T\left\{\frac{G_2 V_T(\boldsymbol{F}) G_1^T}{16L}\delta\theta_1 + \frac{V\left(G_1^T\boldsymbol{F}\right)G_2^T}{16L}\delta\theta_2\right\} \tag{42}$$

where operator $V_T(\boldsymbol{x})$ for a three-dimensional vector $\boldsymbol{x}$ and $V(\boldsymbol{y})$ for a four-dimensional vector $\boldsymbol{y}$ are defined as follows:

$$V_T(\boldsymbol{x}) = 2\begin{bmatrix} 0 & -\boldsymbol{x}^T \\ \boldsymbol{x} & \tilde{\boldsymbol{x}} \end{bmatrix} \tag{43}$$

$$V(\boldsymbol{y}) = 2\begin{bmatrix} y_1 & -y_0 & -y_3 & y_2 \\ y_2 & y_3 & -y_0 & -y_1 \\ y_3 & -y_2 & y_1 & -y_0 \end{bmatrix} \tag{44}$$

Substitution of Eq. (44) into Eq. (34) yields a geometric stiffness as follows:

$$K_{xx}^{Gb} = \frac{E}{16}\int_L \left\{\delta\theta_1^T \quad \delta\theta_2^T\right\}$$

$$\times\begin{bmatrix} -V\left(G_2^T\boldsymbol{F}\right)G_1^T & -G_1 V_T(\boldsymbol{F}) G_2^T \\ G_2 V_T\left(\boldsymbol{F}\right)G_1^T & V\left(G_1^T\boldsymbol{F}\right)G_2^T \end{bmatrix}\begin{Bmatrix}\delta\theta_1 \\ \delta\theta_2\end{Bmatrix} d\boldsymbol{x} \tag{45}$$

It is shown from Eqs. (45) that this geometric stiffness exist only if there is a bending moment in the element $\boldsymbol{F}$ resulting from the first variation of the curvature vector. Thus, derived stiffness matrix is called the bending stabilizing stiffness.

IV. Applications

This section presents computational examples of large deformation analyses on beam structures using DSM. The purpose of the computation is to show that DSM-based finite element analyses provide valid solutions. The first example is a static analysis on a long cantilever subjected to tip moment. The second example is a buckling analysis of a pin supported beam. The third example is the dynamic motion of a flexible beam under pendulum motion.

A. Cantilever Under Tip Moment

The model cantilever is a solid aluminum constant cross section beam whose length is 100 mm and diameter is 1 mm. The undeformed beam is located such that the beam is oriented to the x axis of the global frame. A bending moment is applied at the tip of the beam about the global z axis, and the beam would deform in the xy plane of the global coordinate. The beam was discretized into 10 finite elements (Fig. 3). Young's modulus of the material is 7200 Kgf/mm^2 and the shear modulus is computed by using the residual bending flexibility.[16] The computation was carried out using the arc length control Newton's method with a constant arc length of 100. The deformation profile is shown in Fig. 4. After the computation, good convergence of Newton's method is observed even for largely deformed shapes (Fig. 5). In each incremental stage, the beam deforms with a constant bending curvature. The theoretical relation between the curvature and the applied moment is given as follows:

$$\kappa = M/EI \tag{46}$$

where κ and EI denote the curvature and the bending rigidity, respectively. The computed relation between the curvature and the moment is plotted together with the theoretical relation [Eq. (46)] in Fig. 6. It is shown that the computed result agrees well with

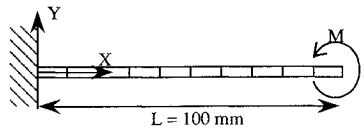

Fig. 3 Cantilever model.

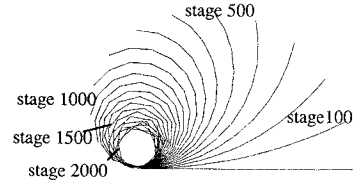

Fig. 4 Cantilever under tip moment.

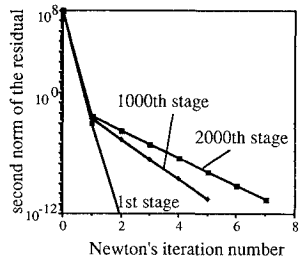

Fig. 5 Newton's method convergence profile.

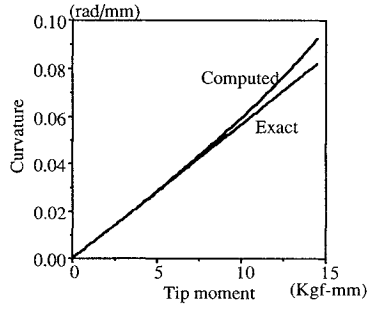

Fig. 6 Curvature in accordance with the moment.

the theoretical solution as long as the curvature is below approximately 0.05 rad/mm, which means that the angular deformation within one element is below 0.5 rad. Deviations are observed when the curvature exceeds this value. This error stems from the curvature approximation of Eq. (15), which essentially represents the angular displacement $\Delta\theta$ between the terminal nodes in an element under single axis rotation,

$$\Delta\theta_a \approx 2\sin(\Delta\theta/2) \tag{47}$$

where $\Delta\theta_a$ represents the approximated deviation. The validity of this approximation is tested (Fig. 7). It is shown that the approximation fails if the angular deformation within an element exceeds about 0.7 rad. This criterion almost agrees with the resultant deformation of one element, 0.5 rad. in the tip-moment analysis. This approximation error limits the proposed method to those problems where the angular deformation in an element is less than 0.5 rad.

B. Euler Buckling of a Pin-Supported Beam

The computational model is a solid aluminum constant cross section beam whose length is 100 mm and diameter is 1 mm. One tip is pin supported to a stationary wall and the other tip is pin supported to a moving wall. The moving wall slides along the global x axis in accordance with the applied compressive force (Fig. 8). The initial shape of the beam has small deformation: 0.50-mm deviation at the midchord and zero deviation at the tips. Elastic moduli are the same as in the preceding example. The computation was carried out by using the arc length control Newton's methods with a constant arc length of 10. The beam was discretized into 10 elements.

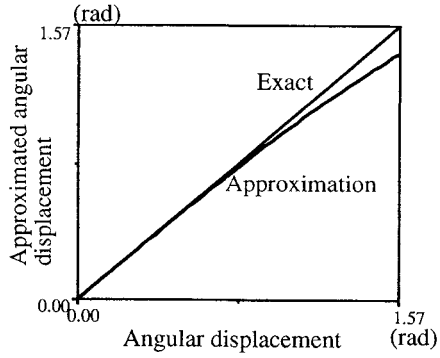

Fig. 7 Angular displacement approximation.

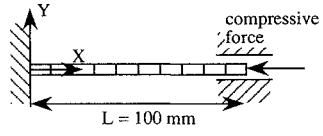

Fig. 8 Buckling analysis model.

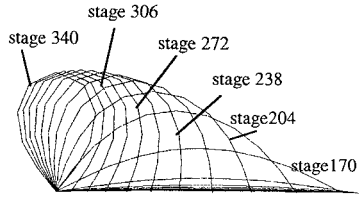

Fig. 9 Deformation profile.

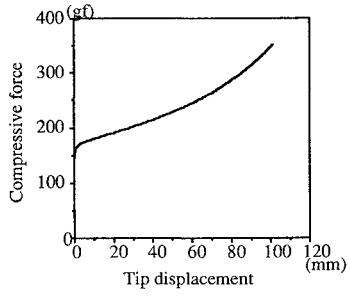

Fig. 10 Pin-supported beam under a compressive force.

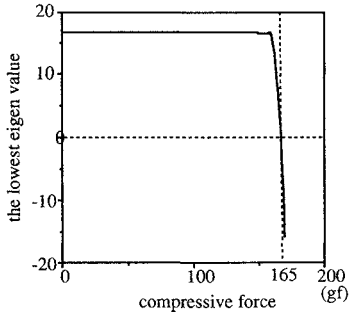

Fig. 11 Fundamental eigenvalue transition in accordance with the applied compression force magnitude.

The deformation profile at each arc length stage is shown in Fig. 9. It is shown that the deformation rapidly grows after the buckling load is attained. The tip displacement in accordance with the applied load magnitude is plotted in Fig. 10. It is shown that the displacement-load relation bifurcates when the applied load exceeds approximately 160 gf. When the applied load is less than 160 gf, the response is hardly observed in the plot since the plot moves almost straight up from the origin along the longitudinal axis. To specify the buckling load, the lowest eigenvalue of the stiffness matrix at the predictor stage of Newton's method is computed (Fig. 11). The lowest eigenvalue reaches zero when the compressive force is 165 gf. After the buckling load is reached, the stiffness matrix becomes

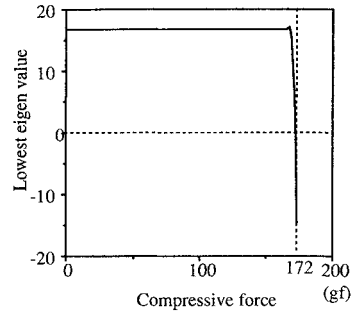

Fig. 12 Fundamental frequency in accordance with the applied moment for small wiggle beam.

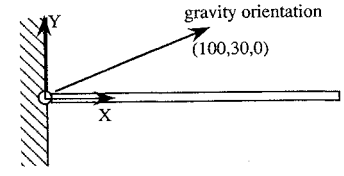

Fig. 13 Elastic pendulum under gravity.

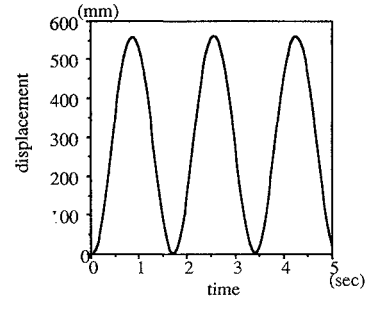

Fig. 14 X displacement of elastic pendulum tip.

indefinite. For verification, the analytical Euler buckling load P was computed as follows:

$$P = n\pi^2(EI/L^2) = 174\,gf \tag{48}$$

Computational results (165 gf) agree with the buckling load within an accuracy of 8%. To clarify the source of the 8% error, the initial deformation is reduced 10 times and the buckling load is recalculated. The fundamental frequency transition, in accordance with the applied moment, is shown in Fig. 12. The zero eigenvalue (buckling load) is reached when the applied moment is approximately 172 gf, which well agrees with the analytical buckling load. The 8% buckling load error for the first computation is, therefore, thought to stem from the initial deformation of the beam.

C. Elastic Pendulum Under Gravity Field

The model beam is a solid aluminum beam of length 1000 mm. In the initial state, the beam lies on the global x axis. The beam experiences a pendulum motion in the x–y plane due to the gravity, which orients (100, 30, 0) in the global coordinate (Fig. 13). Newmark integration is employed to compute the transient response of the pendulum. The x-direction displacement of the tip node (Fig. 14) shows that the fundamental frequency of this pendulum is approximately 0.6 Hz. According to elementary dynamics, the fundamental frequency f of a rigid pendulum of length L is equal to

$$f = \frac{1}{2\pi}\sqrt{\frac{3g}{2L}} \tag{49}$$

where g denotes the gravitational constant. Substituting $g = 9800$ mm/s^2 and $L = 1000$ mm into Eq. (49), the analytical solution is given as $f = 0.61$ Hz, which well agrees with the computed frequency (0.6 Hz). This agreement verifies that the proposed method can well approximate rigid body motion even though the

method does not possess any variable which explicitly represents rigid body motion.

V. Conclusion

Direct strain measure is nonlinear kinematics for the finite element analysis on beam structures under large deformation and finite rotation. Strain components are directly extracted from the current nodal variables: nodal position in the global coordinate system and Euler parameter to describe the rotation from the initial nodal orientation to the deformed nodal orientation. The internal force and the tangent stiffness matrices are derived in a straightforward manner to constitute a Newton's method solution sequence. Computational results indicate that a nonlinear finite element program based on the proposed direct strain measure yields accurate simulations as long as the angular deformation per element is less than 0.5 rad.

References

[1]Atluri, S. N., "Alternate Stress and Conjugate Strain Measures, and Mixed Variational Formulations Involving Rigid Rotations, for Computational Analyses of Finitely Deformed Solids, with Application to Plates and Shells—1," *Computers and Structures*, Vol. 18, No. 1, 1984, pp. 93–116.

[2]Iura, M., and Atluri, S. N., "Dynamic Analysis of Finitely Stretched and Rotated Three-dimensional Space-Curved Beams," *Computers and Structures*, Vol. 29, No. 5, 1988, pp. 875–889.

[3]Iura, M., and Atluri, S. N., "On a Consistent Theory, and Variational Formulation of Finitely Stretched and Rotated 3-D Space-Curved Beams," *Computational Mechanics*, Vol. 4, 1989, pp. 73–88.

[4]Crivelli, L. A., "A Total-Lagrangian Beam Element for Analysis of Nonlinear Space Structures," Ph.D. Thesis, Univ. of Colorado, Boulder, CO, 1991.

[5]Belytschko, T., and Hsieh, B. J., "Non-linear Transient Finite Analysis with Convected Co-ordinate," *International Journal for Numerical Methods in Engineering*, Vol. 7, 1973, pp. 255–271.

[6]Belytschko, T., and Schwer, L., "Large Displacement, Transient Analysis of Space Frames," *International Journal for Numerical Methods in Engineering*, Vol. 11, 1977, pp. 65–84.

[7]Belytschko, T., and Glaum, W., "Applications of Higher Order Corotational Stretch Theories to Nonlinear Finite Element Analysis," *Computers and Structures*, Vol. 10, 1979, pp. 175–182.

[8]Hodges, D. H., "Nonlinear Beam Kinematics for Small Strains and Finite Rotations," *Vertica*, Vol. 11, No. 3, 1987, pp. 573–589.

[9]Hsiao, K. M., and Hou, F. Y., "Nonlinear Finite Element Analysis of Elastic Frames," *Computers and Structures*, Vol. 26, No. 4, 1987, pp. 693–701.

[10]Hsiao, K. M., and Jang, J. Y., "Dynamic Analysis of Planar Flexible Mechanisms by Co-rotational Formulation," *Computer Methods in Applied Mechanics and Engineering*, Vol. 87, 1991, pp. 1–14.

[11]Hsiao, K. M., "Corotational Total Lagrangian Formulation for Three-Dimensional Beam Element," *AIAA Journal*, Vol. 30, No., 3, 1992, pp. 797–804.

[12]Rankin, C. C., and Brogen, F. A., "An Element Independent Corotational Procedure for the Treatment of Large Rotations," *Journal of Pressure Vessel Technology*, Vol. 108, 1986, pp. 165–174.

[13]Mitsugi, J., and Yasaka, T., "Nonlinear Static and Dynamic Analysis Method of Cable Structures," *AIAA Journal*, Vol. 29, No. 1, 1991, pp. 150–152.

[14]Shabana, A. A., *Dynamics of Multibody Systems*, Wiley-Interscience, New York, 1989, Chap. 2.

[15]Nikravesh, P. E., *Computer-Aided Analysis of Mechanical Systems*, Prentice–Hall International, London, 1988, p. 175.

[16]MacNeal, R. H., "A Simple Quadrilateral Shell Element," *Computers and Structures*, Vol. 8, 1978, pp. 175–183.